

Measurement of enhanced spin-orbit coupling strength for donor-bound electron spins in silicon

Radha Krishnan,¹ Beng Yee Gan,¹ Yu-Ling Hsueh,² A.M. Saffat-Ee Huq,² Jonathan Kenny,¹ Rajib Rahman,² Teck Seng Koh,¹ Michelle Y. Simmons,³ and Bent Weber^{1,*}

¹*School of Physical and Mathematical Sciences,*

Nanyang Technological University, 21 Nanyang Link, Singapore 637371

²*School of Physics, University of New South Wales, Sydney, NSW 2052, Australia*

³*Centre for Quantum Computation and Communication Technology,*

School of Physics, University of New South Wales, Sydney, NSW 2052, Australia

1. ABSTRACT

While traditionally considered a deleterious effect in quantum dot spin qubits, the spin-orbit interaction is recently being revisited as it allows for rapid coherent control by on-chip AC electric fields. For electrons in bulk silicon, SOC is intrinsically weak, however, it can be enhanced at surfaces and interfaces, or through atomic placement. Here we show that the strength of the spin-orbit coupling can be locally enhanced by more than two orders of magnitude in the manybody wave functions of multi-donor quantum dots compared to a single donor, reaching strengths so far only reported for holes or two-donor system with certain symmetry. Our findings may provide a pathway towards all-electrical control of donor-bound spins in silicon using electric dipole spin resonance (EDSR).

2. INTRODUCTION

Donor bound electron spins [1, 2] in silicon are promising qubit candidates for the implementation of quantum information processing due to their exceptionally long spin relaxation (T_1) [3] and coherence times (T_2) [4]. This is owing to a low concentration of nuclear spins in the crystalline bulk matrix [4, 5], especially in isotopically enriched ^{28}Si , and generally weak coupling to charge noise due to the weak coupling of the electron's spin to orbital degrees of freedom [6]. For donor spin qubits that are embedded deep within the silicon bulk crystal, far from any interface, inversion asymmetry of the silicon lattice precludes Dresselhaus spin-orbit coupling (SOC), and an isotropic Coulombic confinement potential gives rise to approximately spheroid-symmetric envelope wave functions in the lowest valley-orbit states, allowing for only weak Rashba SOC and higher-order electro-magnetic SOC [7].

Traditionally, SOC has been considered as an undesired effect in spin qubits, as it can dominate spin relaxation [8–10], lead to state leakage through mixing of singlet (S) and triplet (T^-) states [11], or an overall increased sensitivity to charge noise [12]. In turn, however, SOC may be harnessed for rapid electrical control of indi-

vidual spin qubits [13]. Much effort has therefore recently been directed towards driving electric-dipole spin resonance (EDSR) transitions [14, 15] via the Stark shift [16] or by utilizing the disparity in the g -factors [17] for individual addressability of qubits via a microwave field [18–22]. Demonstrations have so far largely been restricted to hole spin qubits bound to silicon quantum dots [23, 24] and acceptor atoms [25, 26] in which SOC-mediated enhanced coupling to external AC electric fields [27, 28] may be combined with long spin life- [29] and coherence times [30]. Enhanced SOC, however, has more recently also been reported for electron spin qubits in metal-oxide-semiconductor (MOS) quantum dots [16, 19, 24, 31, 32], as well as in donors [7, 33]. However, the strength of the SOC (~ 100 neV) reported [16, 19, 24, 31, 32] is usually 2-3 orders of magnitude weaker for electrons compared to holes [24, 26] (see Table I).

Several factors have been reported to enhance the weak SOC for electrons in silicon [7, 12, 34]. For instance, electric fields at surfaces or interfaces, such as Si/SiO₂ [35] or SiGe/Si [34], can enhance Rashba SOC [36], while breaking of mirror symmetry and atomic-scale roughness of interfaces has been shown to produce a significant Dresselhaus SOC contribution [12]. In donor-based systems, strong electric fields can displace the electron wave function from the donor nucleus and can give rise to electric field-induced SOC [7]. Also, engineering two donor atoms at specific locations can change local symmetry and result in both Rashba and Dresselhaus SOC [33]. For hole spins, SOC is known to be strongly enhanced, owing to the reduced symmetry of the non-spheroid spin carrier wave function [37].

Similarly, as we show in this work, SOC can be significantly enhanced by more than 2 orders of magnitude for electrons in multi-donor quantum dots due to an interplay of the atomically-sharp confinement potential with dopant placement disorder, a small valley-orbit splitting and non-spherical manybody wave functions. We draw our conclusions from the transport spectroscopy of a multi-donor double quantum dot in the Pauli spin blockade regime, in which a pronounced leakage is observed at the degeneracy point of the effective valence spin singlet $S(0, 2)$ and triplet $T^-(1, 1)$ states. A transport model of spin-dependent second-order tunneling confirms that

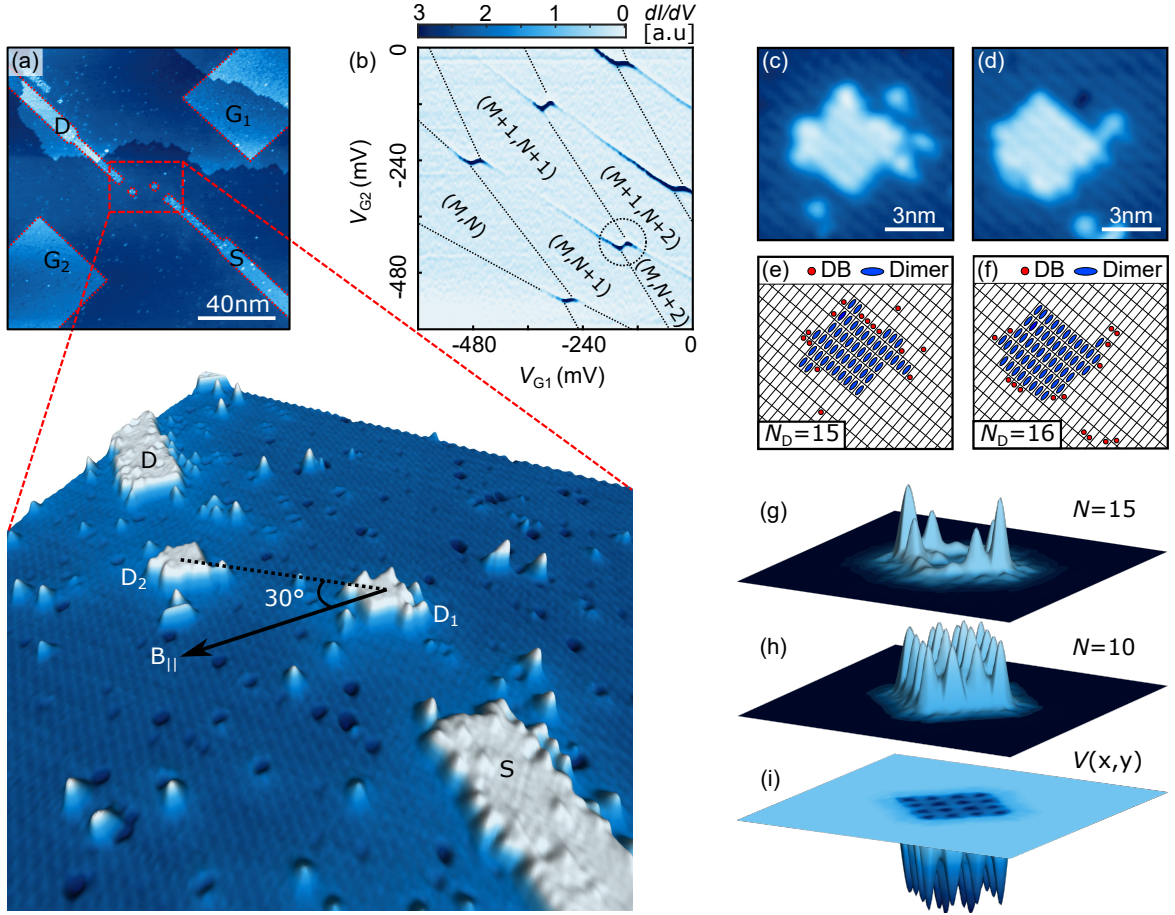


FIG. 1. **Si:P DQD Device.** (a) Overview STM-image after hydrogen resist lithography, showing two quantum dots ($D_{1,2}$), connected to source (S), drain (D), and gate ($G_{1,2}$) electrodes. (b) The charge stability diagram of the DQD shows a number of closed honeycomb domains, where (M, N) indicate the effective electron occupation. (c,d) Atomic-resolution STM images of the two quantum dots allowing to estimate the approximate number of incorporated P donors (e,f). (g-i) Self-consistent confinement potential (i) and tight-binding wave-functions, calculated for the $N = 15$ (g) and $N = 10$ (h) charge state in NEMO-3D.

this resonance can only be explained by an SOC mediated coupling of the singlet and triplet states, while atomistic tight-binding calculations [38] confirm the magnitude of the SOC observed.

TABLE I. **Spin-orbit interaction strength for electrons and holes in silicon.**

Reference	Carrier	SOC strength
Harvey-Collard et al. [31]	Electron	(113 ± 22) neV
Tanttu et al. [32]	Electron	~ 113.73 neV
Jock et al. [35]	Electron	~ 82.7 neV
Weber et al. [7]	Electron	~ 1.05 μ eV
Hsueh et al. [33]	Electron	33.9 μ eV
Li et al. [24]	Hole	110 μ eV
Heijden et al. [26]	Hole	(36 ± 5) μ eV
This Work	Electron	(40 ± 10) μ eV

3. RESULTS AND DISCUSSION

The multi-donor double quantum dot device is shown in Fig.1a, fabricated by STM hydrogen resist lithography [39]. Both quantum dots D_1 and D_2 are ~ 4 nm in diameter, separated by 17.5 ± 0.5 nm (centre to centre), each containing approximately $N_D \simeq 15$ phosphorus (P) donors [39] as estimated from the size of the lithographically defined dots (Fig. 1c-f), assuming that six contiguous dimers of the Si(001)- 2×1 surface are required to incorporate a phosphorus atom into the silicon matrix [40]. Both dots are mutually tunnel-coupled and are coupled to source (S) and drain (D) electrodes which have been staggered to allow independent electrostatic control of the individual dots' electrochemical potentials by gate electrodes G_1 and G_2 [39]. A DC magnetic field was applied within the plane of the device, along the Si $\langle 110 \rangle$ direction, i.e. $\sim 30^\circ$ from the axis connecting the two

quantum dots (arrow in Fig. 1a).

Figure 1b shows the measured charge stability diagram, indicating electron numbers N and M per dot. Absolute electron numbers cannot be determined as the dots could not be fully depleted within the accessible gate-voltage range. However, we expect $N, M \approx N_D \simeq 15$ near charge neutrality ($V_{G1} = V_{G2} = 0$ V) [39, 41].

Despite the large electron numbers, we observe well-defined effective two-electron singlet and triplet states as summarized in Fig. 2. A close-up of the charge transition highlighted by the black dashed circle in Fig. 1b is shown in Figure 2a-d, recorded at a low bias of $V_{SD} = \pm 500$ μ V and at two different values of the applied in-plane magnetic field ($B = 0$ T and $B = 6.1$ T). At larger bias, the charge degeneracy (triple) points widen into bias triangles [39], exhibiting conventional Pauli spin blockade (see Supporting Information). Current along the outlines of the charge stable domains at $B = 100$ mT (dashed white lines) arises from higher-order (co-)tunneling.

Current resonances connecting the triple points reflect co-tunneling due to a strong mutual tunnel coupling between the two quantum dots. At finite magnetic fields $B = 6.1$ T (Fig. 2c,d), we observe that the single inter-dot co-tunneling resonance splits into two. This is more clearly observed in the evolution of the co-tunneling current resonances as a function of magnetic field, recorded along the dashed arrow in Fig. 2b, and plotted in Fig. 2f. The corresponding energy eigenspectrum of SOC-perturbed effective $(1, 1)$ and $(0, 2)$ singlet- (S) and triplet- (T) valence spin states [42] is shown in Fig. 2e. For ease of comparison, the data was rescaled with respect to detuning energy ε , assuming a lever arm ($\alpha = 0.08 \pm 0.01$), extracted from the observed bias window (500 μ eV), and with the magnetic field axis inverted. We define zero detuning ($\varepsilon = 0$) where the singlet states $S(1, 1)$ and $S(0, 2)$ are degenerate, and hybridize due to the tunnel coupling t_c . This is visible from a high intensity resonance at low magnetic fields ($B < 1$ T), that is symmetric upon bias reversal.

At finite magnetic field, the degeneracy of the $T(1, 1)$ and $T(0, 2)$ triplet manifold is lifted, resulting in three non-degenerate levels each, split by the Zeeman energy, $\Delta E_Z = S_z g \mu_B B$. Positive detuning lowers the energy of the $(0, 2)$ states, allowing the triplet states to hybridize at $\varepsilon = 1.21$ meV. This resonance becomes only visible at $B \sim 5$ T, when the hybridized T^- states enter the bias window (horizontal arrows in Fig. 2f). As the detuning at which level alignment of $S(1, 1) - S(0, 2)$ and $T(1, 1) - T(0, 2)$ states occurs does not depend on magnetic field, the corresponding transport resonances do not change position. The finite magnetic field also leads to a change in the $(1, 1)$ ground state from singlet to triplet, giving rise to a level crossing of $T^-(1, 1)$ and the $S(0, 2)$ states when $\Delta E_Z > t_c$ at $B \simeq 1$ T. An enhanced occupation probability of the $T^-(1, 1)$ over the $S(1, 1)$ result in a suppression of co-tunneling current into the drain lead,

and can be understood as a manifestation of Pauli spin blockade in the co-tunneling regime [43]. Current at $B \lesssim 1$ T, also reflected in our transport calculations (Fig. 3), likely has its origin in spin-flip co-tunneling with the S lead [44, 45].

At fields $B \gtrsim 1$ T, spin selection rules should prohibit co-tunneling at the $T^-(1, 1) - S(0, 2)$ level crossing. Yet, a fainter but sharp and clear current resonance is observed that shifts linearly as a function of magnetic field. Such current resonance can only be explained by the presence of a spin non-conserving coupling, such as inelastic co-tunneling [43, 47], nuclear hyperfine interaction [48–52], or, spin orbit coupling [8, 9, 31, 53, 54].

Such coupling of $T^-(1, 1) - S(0, 2)$ states as observed can be understood from the formation of spin-orbit perturbed valley-orbit eigenstates [19, 55]. From first-order perturbation theory, the valley-states in each QD can be expressed as admixtures of both spin polarities by virtue of the spin-orbit coupling,

$$|\Downarrow\rangle = |v_i, \downarrow\rangle - \frac{C_{\text{SOC}}}{\Delta E + \frac{1}{2}g\mu_B B} |v_j, \uparrow\rangle + \dots \quad (1)$$

and

$$|\Uparrow\rangle = |v_i, \uparrow\rangle - \frac{C_{\text{SOC}}^*}{\Delta E - \frac{1}{2}g\mu_B B} |v_j, \downarrow\rangle + \dots \quad (2)$$

Here, $E_Z = g\mu_B B$ is the Zeeman energy with the electron g -factor $g \approx 2$, and ΔE is the valley-orbit splitting. $C_{\text{SOC}} = \langle v_j, \uparrow | H_{\text{SOC}} | v_i, \downarrow \rangle$ is the SOC matrix element. The degree of admixture of the spin-valley states thus sensitively depends on the magnitude of the valley-orbit splitting ΔE . Naturally assumed to be large in atomically confined systems, the valley multiplicity in silicon, especially at large charge occupation [39, 56], provides for comparatively small valley-orbit gaps in the range of a few hundred μ eV [56] to a few meV [39], and thus comparable in magnitude to the much larger few-electron quantum dots realized in SiGe or Si MOS [19, 55].

Given that the spin-valley states of the individual quantum dots contain admixtures of both the spin polarities, they further give rise to a coherent coupling between singlet and triplet states across the two quantum dots of magnitude $C_{\text{SOC}}/\sqrt{2}$. At intermediate magnetic fields, where these are ground states, the magnitude of the effective coupling can be estimated from a Schrieffer-Wolff transformation, as

$$t_{\text{SOC}} = t_c C_{\text{SOC}} / \sqrt{2} \left| \frac{1}{\varepsilon - g\mu_B B} - \frac{1}{\varepsilon - \Delta E} \right| \quad (3)$$

This is hence a second order coupling in which $S(0, 2)$ is coupled to $T^-(0, 2)$ via SOC in the occupied dot, and $T^-(0, 2)$ to $T^-(1, 1)$ via tunneling.

We confirm this notion from a transport model in the co-tunneling regime as summarized in Fig. 3 (see Supporting Information for details). Our model reproduces

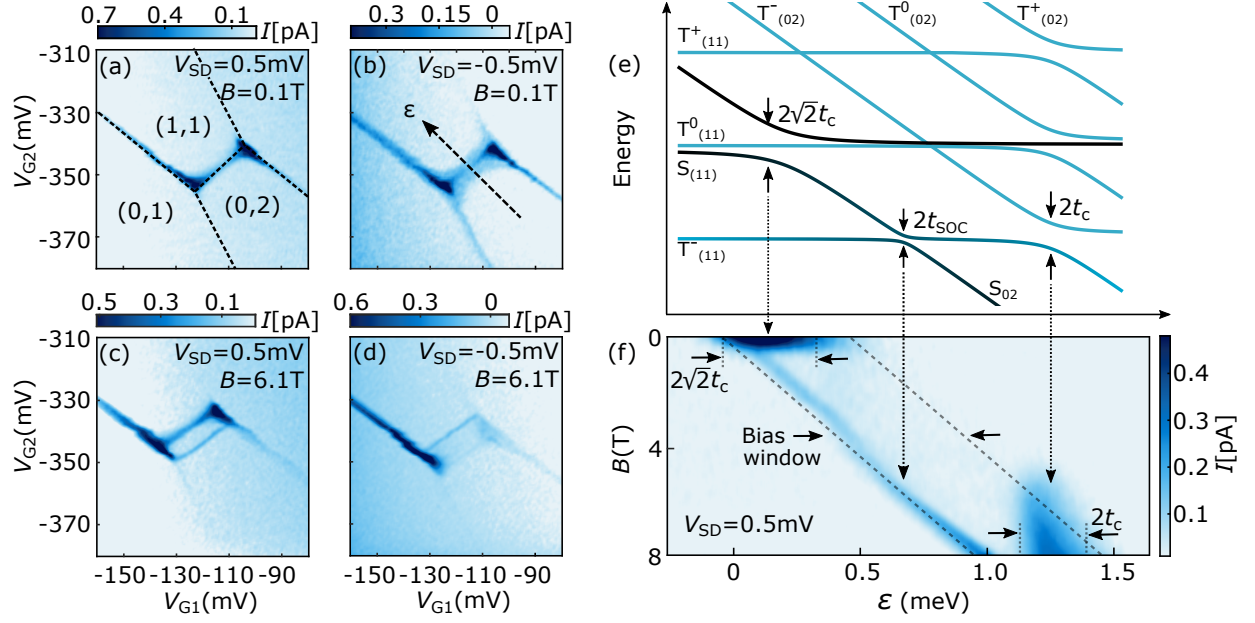


FIG. 2. **Low-bias magnetospectroscopy of the Si:P DQD Device.** (a-d) Close-up of the charge transition highlighted by the dashed circle in Figs. 1b, measured at $V_D = \pm 500 \mu V$, and at $B = 0$ T (a,b) and $B = 6.1$ T (c,d), respectively. (e,f) Co-tunneling current, measured along the dashed arrow in (b) and plotted as a function of magnetic field and detuning, compared to the corresponding energy eigenspectrum (e) of effective two-electron singlet and triplet states. t_c denotes the tunnel coupling, and t_{SOC} the spin-orbit coupling. The bias window is indicated in (f) and the data inverted in B for ease of comparison with (e).

all essential features of the data, but most notably the presence of a single pronounced co-tunneling resonance at intermediate magnetic fields, observed only when the SOC-mediated coupling between the dots is present. This is clearly reflected in the colorplots of Fig. 3a as well as the individual line traces (Fig. 3b) at three different strengths of the magnetic field, comparing the measured drain current with that calculated in second-order transport.

We note that the overall current intensity is dominated by the product of dot-lead tunnel rates Γ_S and Γ_D , while the relative intensities of the respective resonances depend non-linearly on these rates. For example, the current intensity at the singlet resonance observed at low magnetic field (< 1 T) is strongly dependent on dot-lead tunnel rates as it is determined through steady-state DQD populations. Spin blockade occurs when the DQD is in a triplet (1,1) state, lifted by co-tunneling of a spin between a dot and the adjacent lead. Such spin non-preserving processes, in particular spin-flip co-tunneling [44], are therefore implicitly taken into account in the model, but can only explain strong resonant current at $B < 1$ T. For $B > 1$ T, the onset of Pauli spin blockade sets an upper bound on t_c .

Our model also confirms that the resonance lineshapes are Lorentzian when lifetime broadening is dominant. In this case, linewidths and peak intensities are determined by the magnitude of t_c and C_{SOC} . Interestingly, however,

the $S(0,2) - T^-(1,1)$ resonance also possesses a Gaussian character which suggests an inhomogeneous broadening mechanism, for instance due to charge noise in detuning. We can model this by convolving the calculated current (see Supporting Information) with a Gaussian of half-width $\sigma_\epsilon = 17 \mu eV$, in reasonable agreement with recent measurements of bandwidth-integrated charge noise in epitaxial Si:P devices [2, 46]. We note that the current lineshape through the $T^-(1,1) - S(0,2)$ channel is under-determined if both t_c and C_{SOC} are unbounded. However, the upper bound on t_c constrains C_{SOC} from below, which can then be estimated. In a similar way, the upper bound on t_c allows the energy splitting ΔE to be estimated from the lineshape and position of the triplet channel.

From fits to the data, we extract $C_{SOC} \approx 40 \mu eV$, more than two orders of magnitude larger than values previously reported for electrons in silicon, reaching values previously only observed for holes (compare Table I). Such considerable enhancement of the SOC strength likely arises as a combination of several factors, including the atomically-abrupt and disordered Coulombic confinement potential of the dots (Fig. 1h) lowering wave function symmetry and hence increasing the symmetry dependent SOC transition dipole moment [57]. Indeed, we can confirm the magnitude of the SOC strength by atomistic tight-binding calculations of the multi-donor dots, as shown in Fig. 4, plotting C_{soc} against electron occupation

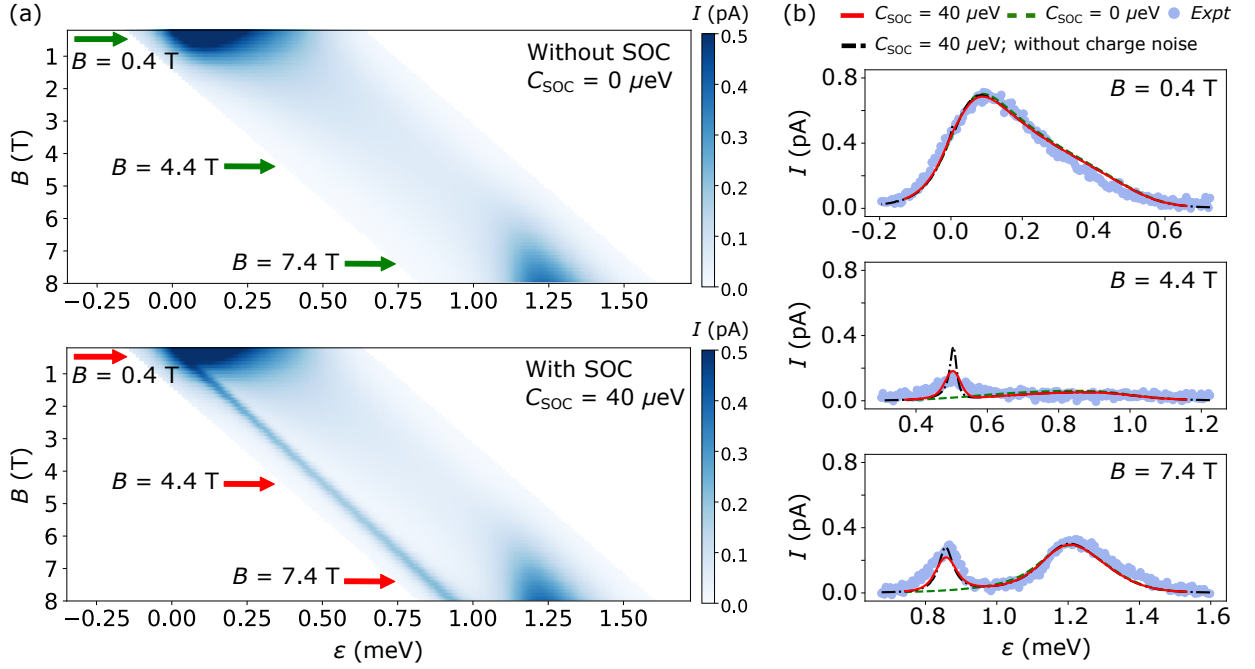


FIG. 3. **Effects of SOC in second order transport.** (a) Second order transport model of the data in Fig. 2, with and without SOC-mediated coherent coupling included (see main text and Supporting Information for detail). No significant co-tunneling current is observed when SOC-mediated coupling is absent while a clear $T^-(1,1) - S(0,2)$ transport resonance is observed in the presence of SOC. (b) Line cuts comparing experiment (Fig. 2f) and theory in terms of resonance line widths and intensities of for low, intermediate and high fields, as indicated by the red arrows in (a). Red and green lines show our results at $C_{\text{SOC}} = 40$ μeV and 0 μeV , respectively, and with Gaussian (charge) noise of magnitude $\sigma_\epsilon = 17$ μeV [46] in the detuning parameter. We see that the charge noise has the effect of broadening and reducing the intensity of the $S(0,2) - T^-(1,1)$ resonance, as can be seen by comparing to results without charge noise (black dashed line).

N . Sixteen P donors, represented by Coulomb charges each with a cutoff potential capturing the central-cell correction, are placed in the Si crystal within a 4 by 4 nm region. The tight-binding Hamiltonian is set up using 20 atomic orbital sp3d5s* basis including nearest-neighbor interactions [58]. A self-consistent Hartree method is used to capture the multi-electron wavefunction, which has successfully reproduced the two-electron binding energy in a single donor [59]. The SOC estimates have been extracted from the self-consistent TB wave functions, directly, by considering calculations with spin-orbit ($|\uparrow\rangle, |\downarrow\rangle$) and without ($|v_i, \uparrow\rangle, |v_j, \downarrow\rangle$) by setting the silicon tight-binding spin-orbit parameter to the bulk value [60, 61] or zero, respectively. A projection from the spin-orbit wave function onto the pure orbital basis then gives us C_{SOC} as plotted in Fig. 4, reaching values between 11 μeV ($N = 16$) and 90 μeV ($N = 6$), matching the value extracted from the experiments (40 μeV) in their order of magnitude. For a range of different disordered donor configurations within the dots, we find values ~ 10 -20 μeV at $N \simeq 15$, confirming that these results are relative robust against dopant placement disorder within the dots. While the model slightly underestimates the SOC strength at $N \simeq 15$, a strong enhancement towards

lower electron occupation likely reflects the less effective screening of the Coulombic confinement potential, amplifying the effects of donor disorder and wave function asymmetry.

4. CONCLUSION

To conclude, we have reported a strong enhancement of the spin-orbit coupling (SOC) strength for spins in the manybody wavefunctions of multi-donor silicon quantum dots, with an SOC energy scale as much as 40 μeV – exceeding previous reports for electrons in silicon quantum dots by two orders of magnitude. We explain this enhancement by the abrupt and disordered nature of the Coulombic confinement potential inherent to donor-based quantum dots, reducing wave-function symmetry. Such strongly enhanced SOC in silicon – similar in magnitude to that for holes – may provide a pathway towards all-electrical control of donor-bound spins in silicon by electric dipole spin resonance (EDSR) as well as may enhance coupling of donor spins to superconducting resonators.

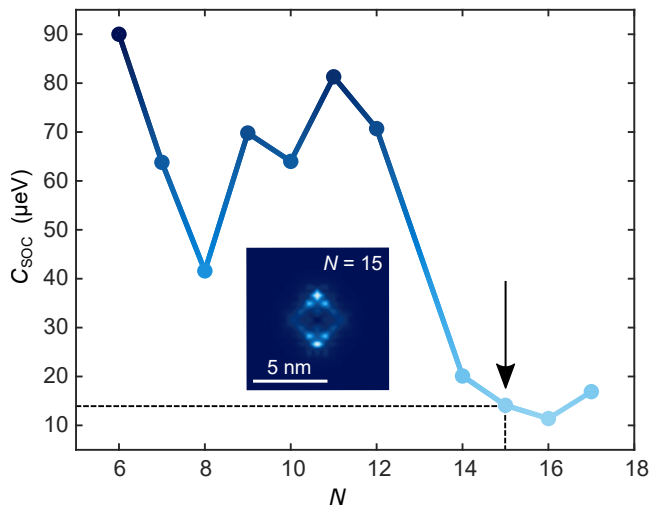


FIG. 4. **Calculated SOC strength.** Strength of the spin-orbit coupling C_{SOC} as calculated from atomistic tight-binding, and plotted as function of the electron number N . The decrease of the SOC strength towards higher electron numbers likely reflects screening of the donor-based Coulombic confinement potential. Insert shows the envelope wavefunction for $N = 15$.

ACKNOWLEDGEMENTS

This research is supported under the Singapore Quantum Engineering Programme (QEP2.0) “Atomic Engineering of Donor-based Spin Qubits in Silicon” (NRF2021-QEP2-02-P07). BW acknowledges a Singapore National Research Foundation (NRF) Fellowship (NRF-NRFF2017-11).

* b.weber@ntu.edu.sg

- [1] T. F. Watson, S. G. J. Philips, K. E., D. R. Ward, S. P., V. M., D. E. Savage, M. G. Lagally, M. Friesen, M. A. Coppersmith, S. N. Eriksson, and V. L. M. K., “A programmable two-qubit quantum processor in silicon,” *Nature*, vol. 555, pp. 633–637, 2018.
- [2] Y. He, S. K. Gorman, D. Keith, L. Kranz, J. G. Keizer, and M. Y. Simmons, “A two-qubit gate between phosphorus donor electrons in silicon,” *Nature*, vol. 571, no. 7765, p. 371, 2019.
- [3] T. F. Watson, B. Weber, Y.-L. Hsueh, L. C. Hollenberg, R. Rahman, and M. Y. Simmons, “Atomically engineered electron spin lifetimes of 30 s in silicon,” *Science Advances*, vol. 3, no. 3, p. e1602811, 2017.
- [4] W. M. Witzel, M. S. Carroll, A. Morello, Ł. Cywiński, and S. D. Sarma, “Electron spin decoherence in isotope-enriched silicon,” *Physical Review Letters*, vol. 105, no. 18, p. 187602, 2010.
- [5] M. Veldhorst, J. Hwang, C. Yang, A. Leenstra, B. de Ronde, J. Dehollain, J. Muhonen, F. Hudson, K. M. Itoh, A. Morello, et al., “An addressable quantum dot qubit with fault-tolerant control-fidelity,” *Nature Nanotechnology*, vol. 9, no. 12, p. 981, 2014.
- [6] F. A. Zwanenburg, A. S. Dzurak, A. Morello, M. Y. Simmons, L. C. Hollenberg, G. Klimeck, S. Rogge, S. N. Coppersmith, and M. A. Eriksson, “Silicon quantum electronics,” *Reviews of Modern Physics*, vol. 85, no. 3, p. 961, 2013.
- [7] B. Weber, Y.-L. Hsueh, T. F. Watson, R. Li, A. R. Hamilton, L. C. Hollenberg, R. Rahman, and M. Y. Simmons, “Spin-orbit coupling in silicon for electrons bound to donors,” *npj Quantum Information*, vol. 4, no. 1, pp. 1–5, 2018.
- [8] Y. Song and S. D. Sarma, “Spin-orbit coupling induced two-electron relaxation in silicon donor pairs,” *Physical Review B*, vol. 96, no. 11, p. 115444, 2017.
- [9] P. Scarlino, E. Kawakami, P. Stano, M. Shafiei, C. Reichl, W. Wegscheider, and L. Vandersypen, “Spin-relaxation anisotropy in a gaas quantum dot,” *Physical Review Letters*, vol. 113, no. 25, p. 256802, 2014.
- [10] J. I. Climente, C. Segarra, and J. Planelles, “Spin-orbit-induced hole spin relaxation in inas and gaas quantum dots,” *New Journal of Physics*, vol. 15, no. 9, p. 093009, 2013.
- [11] D. Stepanenko, M. Rudner, B. I. Halperin, and D. Loss, “Singlet-triplet splitting in double quantum dots due to spin-orbit and hyperfine interactions,” *Physical Review B*, vol. 85, no. 7, p. 075416, 2012.
- [12] R. Ferdous, K. W. Chan, M. Veldhorst, J. Hwang, C. Yang, H. Sahasrabudhe, G. Klimeck, A. Morello, A. S. Dzurak, and R. Rahman, “Interface-induced spin-orbit interaction in silicon quantum dots and prospects for scalability,” *Physical Review B*, vol. 97, no. 24, p. 241401, 2018.
- [13] S. Nadj-Perge, S. Frolov, E. Bakkers, and L. P. Kouwenhoven, “Spin-orbit qubit in a semiconductor nanowire,” *Nature*, vol. 468, no. 7327, pp. 1084–1087, 2010.
- [14] M. Shafiei, K. Nowack, C. Reichl, W. Wegscheider, and L. Vandersypen, “Resolving spin-orbit-and hyperfine-mediated electric dipole spin resonance in a quantum dot,” *Physical Review Letters*, vol. 110, no. 10, p. 107601, 2013.
- [15] E. I. Rashba, “Theory of electric dipole spin resonance in quantum dots: Mean field theory with gaussian fluctuations and beyond,” *Physical Review B*, vol. 78, no. 19, p. 195302, 2008.
- [16] R. Ferdous, E. Kawakami, P. Scarlino, M. P. Nowak, D. Ward, D. Savage, M. Lagally, S. Coppersmith, M. Friesen, M. A. Eriksson, et al., “Valley dependent anisotropic spin splitting in silicon quantum dots,” *npj Quantum Information*, vol. 4, no. 1, pp. 1–8, 2018.
- [17] R. Ruskov, M. Veldhorst, A. S. Dzurak, and C. Tahan, “Electron g-factor of valley states in realistic silicon quantum dots,” *Physical Review B*, vol. 98, no. 24, p. 245424, 2018.
- [18] M. Veldhorst, R. Ruskov, C. Yang, J. Hwang, F. Hudson, M. Flatté, C. Tahan, K. M. Itoh, A. Morello, and A. Dzurak, “Spin-orbit coupling and operation of multi-valley spin qubits,” *Physical Review B*, vol. 92, no. 20, p. 201401, 2015.
- [19] A. Corna, L. Bourdet, R. Maurand, A. Crippa, D. Kotekar-Patil, H. Bohuslavskyi, R. Laviéville, L. Hutin, S. Barraud, X. Jehl, et al., “Electrically driven electron spin resonance mediated by spin-valley-orbit coupling in a silicon quantum dot,” *npj Quantum*

- Information, vol. 4, no. 1, pp. 1–7, 2018.
- [20] W. Huang, M. Veldhorst, N. M. Zimmerman, A. S. Dzurak, and D. Culcer, “Electrically driven spin qubit based on valley mixing,” *Physical Review B*, vol. 95, no. 7, p. 075403, 2017.
 - [21] W. Huang, C. Yang, K. Chan, T. Tanttu, B. Hensen, R. Leon, M. Fogarty, J. Hwang, F. Hudson, K. M. Itoh, et al., “Fidelity benchmarks for two-qubit gates in silicon,” *Nature*, vol. 569, no. 7757, pp. 532–536, 2019.
 - [22] F. Krauth, S. Gorman, Y. He, M. Jones, P. Macha, S. Kocsis, C. Chua, B. Voisin, S. Rogge, R. Rahman, et al., “Flopping-mode electric dipole spin resonance in phosphorus donor qubits in silicon,” *Physical Review Applied*, vol. 17, no. 5, p. 054006, 2022.
 - [23] D. Q. Wang, O. Klochan, J.-T. Hung, D. Culcer, I. Farrer, D. A. Ritchie, and A. R. Hamilton, “Anisotropic pauli spin blockade of holes in a gaas double quantum dot,” *Nano Letters*, vol. 16, no. 12, pp. 7685–7689, 2016.
 - [24] R. Li, F. E. Hudson, A. S. Dzurak, and A. R. Hamilton, “Pauli spin blockade of heavy holes in a silicon double quantum dot,” *Nano Letters*, vol. 15, no. 11, pp. 7314–7318, 2015.
 - [25] R. Maurand, X. Jehl, D. Kotekar-Patil, A. Corna, H. Bohuslavskyi, R. Laviéville, L. Hutin, S. Barraud, M. Vinet, M. Sanquer, et al., “A cmos silicon spin qubit,” *Nature Communications*, vol. 7, no. 1, pp. 1–6, 2016.
 - [26] J. van der Heijden, T. Kobayashi, M. G. House, J. Salfi, S. Barraud, R. Laviéville, M. Y. Simmons, and S. Rogge, “Readout and control of the spin-orbit states of two coupled acceptor atoms in a silicon transistor,” *Science Advances*, vol. 4, no. 12, p. eaat9199, 2018.
 - [27] D. V. Bulaev and D. Loss, “Electric dipole spin resonance for heavy holes in quantum dots,” *Physical Review Letters*, vol. 98, no. 9, p. 097202, 2007.
 - [28] J. Salfi, M. Tong, S. Rogge, and D. Culcer, “Quantum computing with acceptor spins in silicon,” *Nanotechnology*, vol. 27, no. 24, p. 244001, 2016.
 - [29] D. V. Bulaev and D. Loss, “Spin relaxation and decoherence of holes in quantum dots,” *Physical Review Letters*, vol. 95, no. 7, p. 076805, 2005.
 - [30] C. Testelin, F. Bernardot, B. Eble, and M. Chamorro, “Hole-spin dephasing time associated with hyperfine interaction in quantum dots,” *Physical Review B*, vol. 79, no. 19, p. 195440, 2009.
 - [31] P. Harvey-Collard, N. T. Jacobson, C. Bureau-Oxton, R. M. Jock, V. Srinivasa, A. M. Mounce, D. R. Ward, J. M. Anderson, R. P. Manginell, J. R. Wendt, et al., “Spin-orbit interactions for singlet-triplet qubits in silicon,” *Physical Review Letters*, vol. 122, no. 21, p. 217702, 2019.
 - [32] T. Tanttu, B. Hensen, K. W. Chan, C. H. Yang, W. W. Huang, M. Fogarty, F. Hudson, K. Itoh, D. Culcer, A. Laucht, et al., “Controlling spin-orbit interactions in silicon quantum dots using magnetic field direction,” *Physical Review X*, vol. 9, no. 2, p. 021028, 2019.
 - [33] Y.-L. Hsueh, D. Keith, Y. Chung, S. K. Gorman, L. Kranz, S. Monir, Z. Kembrey, J. G. Keizer, R. Rahman, and M. Y. Simmons, “Engineering spin-orbit interactions in silicon qubits at the atomic-scale,” *Advanced Materials*, p. 2312736, 2024.
 - [34] M. Nestoklon, E. Ivchenko, J.-M. Jancu, and P. Voisin, “Electric field effect on electron spin splitting in si ge/si quantum wells,” *Physical Review B*, vol. 77, no. 15, p. 155328, 2008.
 - [35] R. M. Jock, N. T. Jacobson, P. Harvey-Collard, A. M. Mounce, V. Srinivasa, D. R. Ward, J. Anderson, R. Manginell, J. R. Wendt, M. Rudolph, et al., “A silicon metal-oxide-semiconductor electron spin-orbit qubit,” *Nature Communications*, vol. 9, no. 1, pp. 1–8, 2018.
 - [36] S. Lee, H. Koike, M. Goto, S. Miwa, Y. Suzuki, N. Yamashita, R. Ohshima, E. Shigematsu, Y. Ando, and M. Shiraishi, “Synthetic rashba spin-orbit system using a silicon metal-oxide semiconductor,” *Nature Materials*, vol. 20, no. 9, pp. 1228–1232, 2021.
 - [37] S. Liles, R. Li, C. Yang, F. Hudson, M. Veldhorst, A. S. Dzurak, and A. Hamilton, “Spin and orbital structure of the first six holes in a silicon metal-oxide-semiconductor quantum dot,” *Nature Communications*, vol. 9, no. 1, pp. 1–7, 2018.
 - [38] G. Klimeck, S. S. Ahmed, H. Bae, N. Kharche, S. Clark, B. Haley, S. Lee, M. Naumov, H. Ryu, F. Saied, et al., “Atomistic simulation of realistically sized nanodevices using nemo 3-d—part i: Models and benchmarks,” *IEEE Transactions on Electron Devices*, vol. 54, no. 9, pp. 2079–2089, 2007.
 - [39] B. Weber, S. Mahapatra, T. F. Watson, and M. Y. Simmons, “Engineering independent electrostatic control of atomic-scale (4 nm) silicon double quantum dots,” *Nano Letters*, vol. 12, no. 8, pp. 4001–4006, 2012.
 - [40] M. Fuechsle, J. A. Miwa, S. Mahapatra, H. Ryu, S. Lee, O. Warschkow, L. C. Hollenberg, G. Klimeck, and M. Y. Simmons, “A single-atom transistor,” *Nature Nanotechnology*, vol. 7, no. 4, p. 242, 2012.
 - [41] B. Weber, Y. M. Tan, S. Mahapatra, T. F. Watson, H. Ryu, R. Rahman, L. C. Hollenberg, G. Klimeck, and M. Y. Simmons, “Spin blockade and exchange in coulomb-confined silicon double quantum dots,” *Nature Nanotechnology*, vol. 9, no. 6, p. 430, 2014.
 - [42] S. Tarucha, D. Austing, T. Honda, R. Van der Hage, and L. P. Kouwenhoven, “Shell filling and spin effects in a few electron quantum dot,” *Physical Review Letters*, vol. 77, no. 17, p. 3613, 1996.
 - [43] H. Liu, T. Fujisawa, T. Hayashi, and Y. Hirayama, “Pauli spin blockade in cotunneling transport through a double quantum dot,” *Physical Review B*, vol. 72, no. 16, p. 161305, 2005.
 - [44] W. Coish and F. Qassemi, “Leakage-current line shapes from inelastic cotunneling in the pauli spin blockade regime,” *Physical Review B*, vol. 84, no. 24, p. 245407, 2011.
 - [45] N. Lai, W. Lim, C. Yang, F. Zwanenburg, W. Coish, F. Qassemi, A. Morello, and A. Dzurak, “Pauli spin blockade in a highly tunable silicon double quantum dot,” *Scientific Reports*, vol. 1, p. 110, 2011.
 - [46] L. Kranz, S. K. Gorman, B. Thorgrimsson, Y. He, D. Keith, J. G. Keizer, and M. Y. Simmons, “Exploiting a single-crystal environment to minimize the charge noise on qubits in silicon,” *Advanced Materials*, vol. 32, no. 40, p. 2003361, 2020.
 - [47] S. Moriyama, J. Martinek, G. Ilnicki, T. Fuse, and K. Ishibashi, “Inelastic cotunneling mediated singlet-triplet transition in carbon nanotubes,” *Physical Review B*, vol. 80, no. 3, p. 033408, 2009.
 - [48] M. Borhani and X. Hu, “Two-spin relaxation of p dimers in silicon,” *Physical Review B*, vol. 82, no. 24, p. 241302, 2010.
 - [49] A. Johnson, J. R. Petta, J. Taylor, A. Yacoby, M. Lukin, C. Marcus, M. Hanson, and A. Gossard, “Triplet-singlet

- spin relaxation via nuclei in a double quantum dot,” *Nature*, vol. 435, no. 7044, pp. 925–928, 2005.
- [50] J. R. Petta, A. C. Johnson, J. M. Taylor, E. A. Laird, A. Yacoby, M. D. Lukin, C. M. Marcus, M. P. Hanson, and A. C. Gossard, “Coherent manipulation of coupled electron spins in semiconductor quantum dots,” *Science*, vol. 309, no. 5744, pp. 2180–2184, 2005.
 - [51] E. Laird, J. R. Petta, A. C. Johnson, C. Marcus, A. Yacoby, M. Hanson, and A. Gossard, “Effect of exchange interaction on spin dephasing in a double quantum dot,” *Physical Review Letters*, vol. 97, no. 5, p. 056801, 2006.
 - [52] J. R. Petta, J. Taylor, A. Johnson, A. Yacoby, M. Lukin, C. Marcus, M. Hanson, and A. Gossard, “Dynamic nuclear polarization with single electron spins,” *Physical Review Letters*, vol. 100, no. 6, p. 067601, 2008.
 - [53] T. Meunier, I. Vink, L. W. van Beveren, K. Tielrooij, R. Hanson, F. Koppens, H. Tranitz, W. Wegscheider, L. Kouwenhoven, and L. Vandersypen, “Experimental signature of phonon-mediated spin relaxation in a two-electron quantum dot,” *Physical Review Letters*, vol. 98, no. 12, p. 126601, 2007.
 - [54] S. Amasha, K. MacLean, I. Radu, D. Zumbuhl, M. Kastner, M. Hanson, and A. Gossard, “Measurements of the spin relaxation rate at low magnetic fields in a quantum dot,” *arXiv preprint cond-mat/0607110*, 2006.
 - [55] C. Yang, A. Rossi, R. Ruskov, N. Lai, F. Mohiyaddin, S. Lee, C. Tahan, G. Klimeck, A. Morello, and A. Dzurak, “Spin-valley lifetimes in a silicon quantum dot with tunable valley splitting,” *Nature Communications*, vol. 4, no. 1, pp. 1–8, 2013.
 - [56] M. Fuechsle, S. Mahapatra, F. Zwanenburg, M. Friesen, M. Eriksson, and M. Y. Simmons, “Spectroscopy of few-electron single-crystal silicon quantum dots,” *Nature Nanotechnology*, vol. 5, no. 7, p. 502, 2010.
 - [57] C. Tahan and R. Joynt, “Relaxation of excited spin, orbital, and valley qubit states in ideal silicon quantum dots,” *Physical Review B*, vol. 89, no. 7, p. 075302, 2014.
 - [58] G. Klimeck, S. Ahmed, H. Bae, N. Kharche, S. Clark, B. Haley, S. Lee, M. Naumov, H. Ryu, F. Saied, M. Prada, M. Korkusinski, T. Boykin, and R. Rahman, “Atomistic simulation of realistically sized nanodevices using NEMO 3-d—part i: Models and benchmarks,” *IEEE Transactions on Electron Devices*, vol. 54, pp. 2079–2089, Sept. 2007.
 - [59] R. Rahman, G. Lansbergen, J. Verduijn, G. Tettamanzi, S. Park, N. Collaert, S. Biesemans, G. Klimeck, L. Holtenberg, and S. Rogge, “Electric field reduced charging energies and two-electron bound excited states of single donors in silicon,” *Physical Review B*, vol. 84, no. 11, p. 115428, 2011.
 - [60] D. Chadi, “Spin-orbit splitting in crystalline and compositionally disordered semiconductors,” *Physical Review B*, vol. 16, no. 2, p. 790, 1977.
 - [61] T. B. Boykin, G. Klimeck, and F. Oyafo, “Valence band effective-mass expressions in the $sp^3d^5s^*$ empirical tight-binding model applied to a si and ge parametrization,” *Physical Review B*, vol. 69, no. 11, p. 115201, 2004.